



# Fermi National Accelerator Laboratory

FERMILAB-Pub-87/94-A  
June 1987

## Cosmic String Wakes and Large Scale Structure

*Jane C. Charlton*

Dept. of Astronomy and Astrophysics  
University of Chicago

and

NASA/Fermilab Astrophysics Center  
Fermi National Accelerator Laboratory

### *Abstract*

Wakes formed behind infinite strings may be instrumental in large scale structure formation. The production of the dominant wakes, those that could form at  $z \sim 2z_{eq}$  in a Universe dominated by cold dark matter is modeled, and cross-sectional slices through the wake distribution are examined. In a cross section, the cold dark matter wakes tend to outline empty regions with diameters  $(4 - 20 (\Omega_0 h^2)^{-1} Mpc)$  which, for  $h \sim 0.5$ , are not inconsistent with the range of sizes of the voids in the CfA slice of the Universe. The topology of the wake distribution is found to be sponge-like rather than cell-like, thus the empty regions in the cross section are not cuts through spherical voids. Instead, the distribution is an irregular array of intertwining ribbons. Correlations between wakes do not extend much beyond a single horizon at their formation ( $\sim 4 (\Omega_0 h^2)^{-1} Mpc$ ). The fraction of matter that accretes onto wakes is estimated to be between 19% and 83%. If the large scale structure is shaped by wakes the benefit of scale-free correlations of loops is lost, and correlations between clusters of galaxies (extending out to  $\sim 100h^{-1} Mpc$ ) cannot be explained in the context of this model. More extensive three-dimensional surveys should test the large scale structure predictions of the cosmic string wake models.

## I. Introduction

Recently, a great deal of interest has been focused on cosmic strings, largely due to their potential to explain some aspects of large scale structure observations. Much of the effort, to date, has concentrated on the possibility that cosmic string loops naturally generate the correct galaxy-galaxy and cluster-cluster correlation functions (Turok 1985; Szalay and Schramm 1985). In addition, it has been suggested (Vachaspati 1986) that large scale sheets and voids could have been produced when matter fell into wakes formed behind infinite strings. In this paper, the formation of structure from infinite cosmic string wakes is modeled, the topology of the wake system is examined, comparisons are made to the observed shells of galaxies surrounding voids, and the importance of wakes to galaxy formation is explored.

The universe is observed to have structure even on the largest scales that have been mapped. The two-point correlation functions, for galaxies ( $\xi_{gg}(r) \simeq 20(hr)^{-1.8}$ , for  $r \lesssim 10h^{-1}$  Mpc, where, here and throughout, the Hubble parameter is written as  $h = H_0/100 \text{ km s}^{-1} \text{ Mpc}^{-1}$ ) (Groth and Peebles 1977; Shanks *et al.* 1983; Davis and Peebles 1983) and for clusters of galaxies ( $\xi_{cc}(r) \simeq 360(hr)^{-1.8}$ , for  $r \lesssim 100h^{-1}$  Mpc) (Bahcall and Soneira 1983; Klypin and Kopylov 1983), demonstrate that these objects are far from being randomly distributed. For many years people have been aware of long filaments (Chincarini and Rood 1975; Einasto, J  eveer, and Saar 1980; Gregory, Thompson, and Tift 1981; Davis *et al.* 1982; Giovanelli and Haynes 1982) and large voids (Gregory and Thompson 1978; Kirshner *et al.* 1981; Davis *et al.* 1982; Tully 1982). Recently, it has been suggested that such voids may not merely be occasional occurrences, but that in a cross-sectional “slice of the Universe” all galaxies may be on the surfaces of bubble-like structures (deLapparent, Geller, and Huchra 1986). These “bubbles” range in size from  $10h^{-1} - 50h^{-1}$  Mpc in diameter, with an average diameter  $\sim 25h^{-1}$  Mpc.

In a series of papers (Gott, Melott, and Dickinson 1986; Hamilton, Gott, and Weinberg 1986; Gott, Weinberg, and Melott 1987; Weinberg, Gott, and Melott 1987; Melott, Weinberg, and Gott 1987) Gott *et al.* compared the topology generated by various models for structure formation to the CfA redshift survey. The discrete galaxy distribution was smoothed with a Gaussian, and the connectedness of higher and lower density regions was examined. The authors categorized the topology as one of four types: 1) hierarchical, 2) cell-like (or bubble-like), 3) sponge-like (both the high and the low density regions are interconnected), or 4) spaghetti-like (a set of non-intersecting filaments). Gaussian distributions with random phases are a sub-class of the sponge-like topologies, in which the high and low density regions have exactly the same connectedness. Quantitative analysis of topology characterizes structures by their genus (the number of cuts that can be made

without dividing a surface into two pieces). Visual examination of a cross-sectional slice of the Universe is not sufficient to distinguish between a cell-like (bubble) topology and a sponge-like one (in which empty tunnels can resemble circular voids in a cross section). An effective study of the topology of observations requires a larger three-dimensional survey.

Cosmic strings are one-dimensional topological defects, in the orientation of the Higgs field, that might be produced in a symmetry breaking phase transition in the early universe (see, *e.g.*, the review by Vilenkin 1985). In most numerical simulations of string formation random values of the Higgs field are assigned to the vertices of a cubic lattice, and strings pass through a face if the field orientation passes sequentially about the face (Vachaspati and Vilenkin 1984; Albrecht and Turok 1985). Alternatively, Scherrer and Frieman (1986) assign values of the Higgs field to the cells of a tetrakaidekahedral lattice (see Figure 1) so that strings form along lattice edges. The two different lattices yield very similar results. The resulting configuration of strings consists of  $\sim 70\%$ , by length, in infinite strings (those strings that terminate at the boundaries of the lattice). The remainder of the length is in closed loops with a scale-invariant spectrum (Turok 1984; Kibble 1985). ( $n(r) \propto r^{-4} dr$  where  $n$  is the number density of loops with radii between  $r$  and  $r + dr$ .) The network of infinite strings is a collection of Brownian random walks. ( $L \propto d^2/s$  where  $L$  is the length, measured along the string between two points,  $d$  is the distance between the two points, and  $s$  is the segment length.) It is important, however, to note that Brownian correlations only arise between segments on the same infinite string (Scherrer 1987), since the Higgs field is uncorrelated on scales larger than the horizon at formation (approximately the initial segment length). The different Brownian infinite strings are distributed, with respect to each other, in such a way that the overall distribution is random.

The evolution of the cosmic string network has been studied numerically. The equation of motion in a conformal gauge (Turok and Bhattacharjee 1984), where  $\partial/\partial\eta$  is denoted by an overdot,  $\partial/\partial\sigma$  by a prime,  $\sigma$  is the coordinate along the string ( $\vec{x} = \vec{x}(\sigma, t)$ ),  $\eta$  is the conformal time, and  $\epsilon(\sigma, t) = \left[ (\dot{\vec{x}}')^2 / (1 - \dot{\vec{x}}^2) \right]^{1/2}$  is:

$$\ddot{\vec{x}} + 2 \left( \dot{R}/R \right) \dot{\vec{x}} \left( 1 - \dot{\vec{x}}^2 \right) = \frac{1}{\epsilon} \frac{\partial}{\partial\sigma} (\vec{x}'/\epsilon). \quad (1)$$

The second term on the LHS is a damping term, due to the expansion of the universe, and the RHS is a curvature (of the string) term. On scales much greater than the horizon the expansion term dominates, while on smaller scales it can be neglected as compared to the curvature term. Unfortunately, near the horizon scale both terms are significant and equation (1) is not easily solved.

Strings tend to straighten out on the scale of the horizon. When two strings cross the probability of their intercommuting has been calculated (Shellard 1987) to be nearly 1. One

result is the production of a closed loop when an infinite string crosses itself. Also, small loops break off of larger ones. The system of strings seems (Albrecht and Turok 1985,1987) to rapidly approach a scaling solution. In the scaling solution, loops have a scale-invariant spectrum and a two-point correlation function with a slope close to that of galaxies and clusters of galaxies (Turok 1985). This has led to much debate as to whether cosmic string loops are instrumental in galaxy and structure formation (Peebles 1985,1986). The infinite strings remain as a network of Brownian random walks, with segments straightened on the scale  $\lambda = \epsilon t$ , where  $0.7 \leq \epsilon \leq 2$  in the radiation dominated era, and possibly into matter domination, and  $\epsilon \sim 1$  is a most likely value (Turok 1987). The density of the network is:

$$\rho_{IS} = A\mu t^{-2} \quad (2)$$

where  $A \sim 3$  and  $\mu$  is the mass per unit length of the string.

Infinite strings may leave their own mark on the large scale structure of the universe. Vachaspati (1986) has suggested that wakes formed behind infinite strings could become the bubble-like surfaces on which galaxies are distributed. Wakes originate as a result of the deficit angle  $8\pi G\mu$  in the metric of a moving string (Silk and Vilenkin 1984). Physically, matter is attracted towards the string and even when the string has moved past a point, the affected matter collapses into the plane behind the string, thus forming a wake. A recent calculation (Stebbins, *et al.* 1987) shows that, in a Universe dominated by cold dark matter, large scale wake structure is dominated by those wakes formed at  $z \sim 2z_{eq}$ , since they have the highest surface mass density. This agrees with the prediction of Vachaspati (1986). (Wakes formed during radiation domination have their growth damped by the radiation, so they simply dilute due to the expansion of the universe. The surface mass density of wakes in the matter dominated era decreases with  $t^{2/3}$ , so those wakes formed at  $z \sim 2z_{eq}$  sweep up all wakes formed at later times.) In a cold dark matter dominated Universe, the size of a wake is on the order of the comoving horizon size at its formation, ( $\sim 4.1 (\Omega_0 h^2)^{-1} Mpc$  at  $z \sim 2z_{eq}$ ). As a result of the similarity to the size of observed "bubbles", Vachaspati (1986) has suggested that cold dark matter wakes may be important for large scale structure formation. This paper will explore that possibility; however, caution is in order when trying to claim a relationship between the distribution of wakes and the distributions of galaxies and clusters of galaxies. An estimate of accretion in an  $\Omega_0 = 1$  cold dark matter universe has shown that at least 6% of the matter accretes on wakes, but the largest fraction falls onto loops (Stebbins, *et al.* 1987). This issue will be reconsidered, with more attention to the geometry of the wake distribution.

In the following section, the method used to approximate the location of the dominant wakes will be described. Section III presents and interprets illustrations of a cross section

through the wake distribution, and explores the topology and large scale properties of the wake distribution. Section IV is a discussion of the critical issue of whether wakes can be a major factor in large scale structure formation. The results are summarized in Section V.

## II. The Model for Producing the Wake Distribution

The first step in modeling the locations of wakes is to determine the infinite string configuration that produces them. The computer program written by and described in Scherrer and Frieman (1986) was used to determine the initial locations of infinite strings. Their numerical simulation is performed on a tetrakaidekahedral lattice (see Figure 1) rather than the usual cubic lattice (Vachaspati and Vilenkin 1984; Albrecht and Turok 1985). The initial lattice used here is  $240 \times 240 \times 240$ , where the cube in Figure 1 is  $4 \times 4 \times 4$ . Random phases of the Higgs field are assigned to the cells of the lattice (three cells surround each lattice edge) and a string is located on the edge if the assigned phases pass sequentially about the edge. Its direction is defined by the direction in which the phases increase about the edge. The properties of the lattice (four segments intersecting at each vertex) automatically assure that each vertex will either have one string passing in and out, or no string at all. The distribution of open strings resulting from the simulation has density  $\sim 0.2 \epsilon^{-2} \mu t^{-2}$ , where the segment length  $\lambda = \epsilon t = \sqrt{2}$ , and  $\epsilon \sim 1$ . The initial configuration of strings, produced on the tetrakaidekahedral lattice, has a density  $\sim 15$  times smaller than the density reached in the scaling solution (see equation (2)), that should apply at the time ( $z \sim \alpha z_{eq}$  where  $\alpha$  is expected to be of order 2) of dominant wake production. Since a realistic evolved infinite string distribution has a higher density, although it retains the characteristics of a Brownian random walk, the density of the initial configuration must be increased. Clearly the most reliable (but also the most difficult since the horizon scale is the scale of interest) way to do this is to evolve the system using the equation of motion of the strings. However, in this case it is possible to approximate the evolved distribution using a simple model, not intended to be a real time evolution.

The simple model to increase density is illustrated in Figure 2. The infinite strings are “straightened” in steps by simply omitting every other point on each infinite string. Each string remains Brownian and the inter-string correlations are not altered. In a “time-step”, the number of straight segments is halved, and the average segment length is increased by a factor  $F$  that depends upon the discrete angles  $\theta$  between segments. The segment density,  $\rho$ , increases by a factor  $\sim F^3/2$ . Table 1 lists the number of segments, the average segment length, the value of  $F$ , and the segment density,  $n$ , for several “time-steps”.

To find the exact wake locations it would be necessary to solve the equation of motion. Since wakes are produced on the horizon scale, the curvature and damping terms are both

important, and the equation is difficult to solve. An approximate method was devised to give a reasonable idea of the overall distribution. However, this method is not accurate on the scale of single wakes.

The infinite strings, loosely speaking, evolve by straightening out on the horizon scale, and a wake forms along the string trajectory. In the ribbon model, used here, the wake distribution is approximated by the set of triangular planes formed with every set of three adjacent vertices along the string as triangle vertices (see Figure 3). This model should outline the wake distribution, although in reality the “ribbon” should be smoother, and could differ in surface area by up to approximately a factor of two.

### III. Results: Slices Through the Wake Distribution, Topology, and Large Scale Structure

Throughout this section, results will be discussed in the context of cold dark matter wakes, formed at  $z \sim 2z_{eq}$ . An extension to the case of baryon or hot dark matter wakes will be addressed in a separate paper (Charlton 1987). As a first step towards evaluating the promise of wakes in explaining large scale structure, slices of the wake distribution have been examined. Figures 4a-c are cross sections of the wake distribution formed at the times when the infinite string network had densities 0.40, 1.2, and  $2.5\epsilon^{-2}\mu t^{-2}$ . The later density is probably the closest to that at the time of dominant wake production. The average segment length of the infinite string network,  $\lambda = \epsilon t$ , is marked on each figure. (The horizon size is  $t/(1-n)$ , where the scale factor  $a \propto t^n$ , but here the length of a straight string segment,  $\lambda = \epsilon t$ , is the more relevant parameter.) Empty regions are apparent in the cross sections, ranging from 1-5  $\lambda$  in diameter. This qualitative result is not expected to be altered for higher values of  $\epsilon$ . The value of  $\lambda$  at  $z = \alpha z_{eq}$  is:

$$\lambda = c \epsilon t(\alpha z_{eq}) = \frac{2}{3} \epsilon \Omega_0^{-1/2} \frac{c}{H_0} z_{eq}^{-3/2} \left[ \frac{(1-2\alpha)(1+\alpha)^{1/2}}{\alpha^{3/2}} + 2 \right]. \quad (3)$$

Using  $z_{eq} = 2.5 \times 10^4 (\Omega_0 h^2)$  and  $c/H_0 = 3000 h^{-1} Mpc$ ,  $\lambda$  corresponds to a present scale of

$$\begin{aligned} \lambda(\alpha z_{eq}) &= z_{eq} c \epsilon t(\alpha z_{eq}) = 12.6 \epsilon (\Omega_0 h^2)^{-1} \left[ \frac{(1-2\alpha)(1+\alpha)^{1/2}}{\alpha^{3/2}} + 2 \right] Mpc \\ &= 4.1 \epsilon (\Omega_0 h^2)^{-1} Mpc, \quad \alpha = 2 \\ &= 7.4 \epsilon (\Omega_0 h^2)^{-1} Mpc, \quad \alpha = 1 \end{aligned} \quad (4)$$

Thus the empty regions in the figure range from  $4-20 \epsilon (\Omega_0 h^2)^{-1} Mpc$  in diameter. Figure 5 is a portion of Figure 4c drawn to the scale of the CfA slice for  $\epsilon \sim 1$  (de Lapparent, Geller, and Huchra 1986), with the choices  $h = 0.5$  and  $h = 1$ . The larger sizes of the

voids in the  $h = 0.5$  case appear more consistent with the observations. Note that a larger  $\epsilon$  would have the same effect as a decrease in  $h$ .

The task of determining the topology of the wake distribution differs somewhat from a topological study of the galaxy distribution, in which the points must be smoothed to form surfaces. Here the distribution of the wake surfaces themselves will be examined. It is really the topology of the smoothed galaxy distribution, that could potentially be shaped by the wake surfaces in this model, that should be compared to the topology of the observed galaxy distribution. The wake distribution is a network of intertwined ribbons. Since the ribbons are interconnected high density surfaces, the topology cannot be hierarchical. It can easily be determined if these ribbons close around cells, or whether the topology is sponge-like. It is clear, from Figure 4 alone, that the wake surfaces do not completely close around three dimensional voids, since there are very few closed regions even in the two dimensional slices. Strictly speaking, the topology is sponge-like, but not Gaussian. A study of the properties of the three-dimensional distribution can, however, add crucial information.

Figure 6 is a picture of the three-dimensional wake distribution in a cube with a side  $2\lambda$  in length. The shapes of the empty regions can be probed with plots of the distance to nearest neighbors in various directions from a randomly chosen point. Figures 7a-c plot the distances to nearest neighbors in 360 equally spaced directions in in each of three perpendicular planes. These can be compared to similar curves (Figures 7d-e) for points interior to closed spheres and cubes. The voids in the wake distribution are much more irregular than spherical or cubical voids, with empty tubes extending through many horizon lengths in some directions.

The sizes of empty regions are probed in Figure 8, a graph of the probability that a region of radius  $r$  about a randomly chosen point is empty vs.  $r$ . This probability is derived from

$$p(r) = \int_r^\infty N_s(r) dr \quad (5)$$

where  $N_s(r)$  is the probability that the nearest neighbor is at a distance between  $r$  and  $r + dr$ , found by determining the distance to the nearest wakes from 5000 different randomly selected locations. (See White, *et al.* 1987 for a discussion of this and other related statistics in connection with large scale structure in a cold dark matter model.) For comparison, a Poisson distribution of points with a density,  $n$ , equal to that of the triangular wake planes ( $p(r) = \exp[-(4\pi/3)r^3n]$ ) is also considered in Figure 8. As would be expected, the probability that a region at small  $r$  is empty is smaller for wakes than for a Poisson distribution of points. The third curve in Figure 8 is the probability that a region of radius  $r$  in a cross section is empty. The empty spherical regions are smaller than the

empty circular regions in the cross section.  $p(r)$  drops nearly to 0 beyond a radius of about  $\lambda/2$ , thus there are few spherical regions with radii greater than  $4.1 \epsilon (\Omega_0 h^2)^{-1} Mpc$ . The empty regions in the wake distribution are not evenly spaced, roughly spherical voids, but are very irregular in shape.

A final large scale consideration is the correlation function between wakes. Due to the motions of the strings, correlations develop on scales up to the horizon at any given time. On scales larger than the horizon at wake production, the amplitude of the correlation function between either central or randomly chosen points, one on each triangular wake region, drops to zero. This is as would be expected, since the orientation of the Higgs field was uncorrelated on scales larger than the correlation length at formation. As a very rough illustration of the correlations between galaxies on wakes, an average of ten randomly located points on each triangular wake section are chosen. (The number of points chosen on each wake is proportional to the area of the wake surface.) These points represent objects that are probably more massive than galaxies, since each triangular wake weighs  $\sim 5 \times 10^{12} h^{-2} M_\odot$ . Figure 9 is a plot of the correlation function for initial infinite string density  $2.5 \epsilon^{-2} \mu t^{-2}$ , setting the distance  $\lambda = 4.1 \epsilon (\Omega_0 h^2)^{-1} Mpc$  equal to the average segment length. At small separations the slope of the  $\log \xi$  vs.  $\log r$  curve approaches  $-1$  as is expected for a random distribution of points on a plane. Of course in a realistic situation this slope could be drastically altered, due to the rearrangement (gravitational and explosive) that would take place on small scales. At large separations, exceeding the average interwake spacing, the amplitude drops to zero. The distance at which the amplitude drops to zero corresponds to  $\sim 5.7 \epsilon (\Omega_0 h^2)^{-1} Mpc$ , or  $11.4 h^{-1} Mpc$  for  $\epsilon \sim 1$ ,  $\Omega_0 = 1$ , and  $h = 0.5$ . This compares to the distance to which galaxies are observed to be correlated ( $\sim 10 h^{-1} Mpc$ ), but only for a much smaller  $\Omega_0$  (that would produce much larger voids) could correlations extend to the scale of clusters of galaxies ( $\sim 100 h^{-1} Mpc$ ).

#### IV. Relevance of Wakes to the Distribution of Galaxies

We have seen in the previous section that the cold dark matter wake distribution has some features in common with the observed galaxy distribution. Is this merely a coincidence, or do wakes in some way become the sites of galaxies? Schemes for galaxy formation on wakes fall into three general categories: 1) Galaxies form from fragmentation of baryonic wakes (Rees 1986). (After  $z_{rec}$  the baryon sound speed drops sufficiently to allow collapse of the baryons into the cold dark matter wakes discussed in the previous section.) After radiative cooling, gravitational instability of these baryon-cold dark matter wakes may have yielded a generation of Population III massive stars or supermassive objects. These objects could provide seeds for an explosive galaxy formation scenario (Ostriker and Cowie 1981) on the wake surfaces; 2) Galaxies form around loops which fall

into the wakes (Vachaspati 1986; Stebbins, *et al.* 1987); 3) Loops form near or fall into the wakes, and provide seeds for galaxy formation within the wake. These three possibilities have been mentioned by Peebles (1986).

A major complication in all of these schemes is the potential competition between loops and wakes, and the possible dominance of loops. The fraction accreting onto the wakes can be estimated here with a more correct modeling of the geometry of the wake distribution than in Stebbins, *et al.* (1987). The maximum width of a wake at  $z \sim 2z_{eq}$  from Stebbins, *et al.* (1987) is  $3 \Omega_0^{1/2} Mpc$  for  $G\mu \sim 10^{-6}$ , and momentum  $\beta_s \gamma_s = 1$ , where  $\beta_s = v/c$  and  $\gamma_s = (1 - \beta_s^2)^{-1/2}$ . Therefore, for  $\Omega_0 = 1$ , matter within  $1.5 Mpc$  of any wake (a fraction  $1 - p(1.5 Mpc)$  given in Figure 8) could be swept up. Certainly some, or most, of the mass within this region could accrete onto the loops, but the loops themselves would be affected by wakes, and some would fall in. Thus this estimate is a maximum fraction that could accrete onto wakes. In an  $\Omega_0 = 1$  cold dark matter Universe, this fraction is 19% for  $h = 0.5$ , and 83% for  $h = 1$  (using  $\lambda = 4.1 (\Omega_0 h^2)^{-1} Mpc$ ). These compare to a fraction  $24 f \mu_6 \beta_s^2 \gamma_s^2 h^2 \%$  estimated in Stebbins, *et al.* (1987), where  $f$  is the ratio of the length in infinite strings to the horizon length,  $\mu_6$  is  $G\mu$  in units of  $10^{-6}$  and  $\beta_s \gamma_s$  is the momentum. The two estimates are comparable for the value,  $f \sim 2.5$ , that is consistent with the density of the infinite strings that produced the wake distribution described in Figure 8. The fraction accreting onto wakes is clearly highly dependent upon the parameters of the problem, hence it is not clear how wakes figure in galaxy formation.

Even if the largest fraction of matter does accrete onto loops, it is still quite possible that wakes are important for galaxy formation. Stebbins *et al.* (1987) showed that the dominant wakes are not disrupted by the presence of loops, even though the loops may have accreted the majority of the matter. Instead, the condensations that form around the loops can fall into the wakes. They suggested that the most luminous galaxies are more likely to form about loops in overdense regions like wakes. Thus the wakes could provide a natural biasing mechanism. This scheme suggests that voids are not empty, but contain lower luminosity galaxies.

## V. Summary and Conclusion

A cross section through the cold dark matter wake distribution, produced with the ribbon model, has empty regions  $4 - 20 \epsilon (\Omega_0 h^2)^{-1} Mpc$  in diameter. This cross section roughly resembles the CfA slice of the Universe for  $h \sim 0.5$ , and  $\epsilon \sim 1$ . Of course, to relate the wake locations to the sites of galaxies would require a specific model for galaxy formation, and a knowledge of wake dynamics on small scales, not addressed by the ribbon model.

The wake distribution itself has sponge-like, rather than cell-like topology. The wake

surfaces do not close completely, even in the two-dimensional slices. Looking in some directions, from a randomly chosen point, there are gaps in the wake distribution, and no wakes are seen for many horizons. Also, the probability of having an empty three-dimensional spherical region drops nearly to zero beyond a diameter of  $4 \epsilon (\Omega_0 h^2)^{-1} \text{ Mpc}$ . The empty regions seen in the cross sections of the wake distribution are not simply cuts through spherical voids. This is an important prediction of a cosmic string wake galaxy formation model.

Correlations between cold dark matter wakes do not extend much beyond a horizon length at  $z_{eq}$  ( $\sim 4 \epsilon (\Omega_0 h^2)^{-1} \text{ Mpc}$ ) so it is unlikely that cold dark matter wakes are responsible for the correlations between clusters of galaxies. However, it is conceivable that they could reproduce observed galaxy-galaxy correlations.

An estimate of the fraction of matter to accrete onto cold dark matter wakes indicates that wakes could be more important in galaxy formation than previously anticipated, although this depends largely upon the parameters of the problem ( $\Omega_0$ ,  $h$ , horizon size at wake formation, wake thickness, etc.). For  $h = 0.5$  (the most appropriate choice for matching the CFA slice) the fraction to accrete onto wakes is 19% in accord with the previous estimate (Stebbins, *et al.* 1987). It also depends upon the galaxy formation scheme (*e.g.*, the wakes themselves fragment to form galaxies, galaxies form around loops that later fall into wakes, or loops fall into wakes and galaxies form around them).

Models of galaxy formation involving cosmic string wakes, and their consequences on large scale structure, have not been explored as rigorously as have many other models for structure formation, such as cold or hot dark matter models. This is largely because a detailed analysis requires committal to a specific model of galaxy formation on wakes, that would involve loops, wakes, some variety of dark matter, and numerous uncertain parameters. One point of view is the potentially disruptive effect that wakes could have on the model of galaxy formation around loops of cosmic string. The most striking feature of cosmic string schemes of galaxy formation is the scale-free correlations, naturally generated by loops. If wakes are indeed influential in shaping large scale structure, they will destroy the correlations between the loops that fall into wakes. So wakes may be looked upon as an undesirable feature of cosmic string models, that must be ruled out for their success. On the other hand, general large scale structure considerations indicate that wakes may be of interest. As more extensive three-dimensional observational surveys become available, the predictions of wakes for topology and void sizes can be tested. If the results are favorable, specific models can be devised and their consequences explored.

## Acknowledgements

I would like to thank A. Albrecht, D. Bennett, A. Melott, A. Stebbins, N. Turok, T. Vachaspati, and many other participants at the Cosmic String Workshop at Fermilab for useful discussions. I am especially grateful to my advisor D. Schramm, to M. Turner for his careful reading of the manuscript, and to R. Scherrer for his comments and the use of his computer code. Computing was done on the Cray XMP at the National MFE Computing Center at Livermore as sponsored by the astrophysics group at Fermilab. This work was supported by the NSF at the University of Chicago.

**Table 1: Parameters for Model to Increase Density**

Timesteps completed	Number of segments	Av. seg. length	F	$(\xi^{-2}\rho\mu t^{-2})$
0	$9 \times 10^5$	1.41	...	0.20
1	$4.5 \times 10^5$	2.31	1.63	0.40
2	$2.2 \times 10^5$	3.61	1.56	0.76
3	$1.1 \times 10^5$	5.36	1.49	1.2
4	$5.4 \times 10^4$	7.75	1.45	1.8
5	$2.6 \times 10^4$	11.0	1.42	2.5
6	$1.2 \times 10^4$	15.5	1.41	3.3

## References

- Albrecht, A., and Turok, N. 1985. *Phys. Rev. Lett.*, **54**, 1868.
- Albrecht, A., and Turok, N. 1987, in preparation.
- Bahcall, N.A., and Soneira, R.M. 1983, *Ap. J.*, **270**, 20.
- Charlton, J.C. 1987, in preparation.
- Chincarini, G., and Rood, H.J. 1975, *Nature*, **257**, 294.
- Davis, M., Huchra, J., Latham, D.W., and Tonry, J. 1982, *Ap. J.*, **253**, 423.
- Davis, M., and Peebles, P.J.E. 1983, *Ap. J.*, **267**, 465.
- de Lapparent, V., Geller, M., and Huchra, J.P. 1986, *Ap. J.*, **302**, L1.
- Einasto, J., Jõeveer, M., and Saar, E. 1980, *MNRAS*, **193**, 353.
- Giovanelli, R., and Haynes, M.P. 1982, *A. J.*, **87**, 1355.
- Gott, J.R., Melott, A.L., and Dickinson, M. 1986, *Ap. J.*, **306**, 341.
- Gott, J.R., Weinberg, D., and Melott, A.L. 1986, *Ap. J.*, in press.
- Gregory, S.A., and Thompson, L.A. 1978, *Ap. J.*, **222**, 784.
- Gregory, S.A., Thompson, L.A., and Tifft, W.G. 1981, *Ap. J.*, **243**, 411.
- Groth, E.J., and Peebles, P.J.E. 1977, *Ap. J.*, **217**, 385.
- Hamilton, A.J.S., Gott, J.R., and Weinberg, D. 1986, *Ap. J.*, **309**, 1.
- Kibble, T.W.B. 1985, *Nucl. Phys.*, **B252**, 227.
- Kibble, T.W.B., and Turok, N. 1982, *Phys. Lett.*, **116B**, 141.
- Kirshner, R.P., Oemler, A., Schechter, P.L., and Schectman, S.A. 1981, *Ap. J.*, **248**, L57.
- Klypin, A.A., and Kopylov, A.I. 1983, *Sov. Astron. Lett.*, **9**, 41.
- Melott, A.L., Weinberg, D., and Gott, J.R. 1987, *Ap. J.*, submitted.
- Ostriker, J.P., and Cowie, L.L. 1981, *Ap. J.*, **243**, L127.
- Rees, M.J. 1986, *MNRAS*, **222**, 27P.
- Peebles, P.J.E. 1985, "Screed I", unpublished.
- Peebles, P.J.E. 1986, "Screed II", unpublished.
- Scherrer, R.J. 1987, *Ap. J.*, in press.
- Scherrer, R.J., and Frieman, J.A. 1986, *Phys. Rev. D*, **33**, 3556.
- Shanks, T., Bean, A.J., Efstathiou, G., Ellis, R.S., Fong, R., and Peterson, B.A. 1983, *Ap. J.*, **274**, 529.
- Shellard, E.P.S. 1987, *Nucl. Phys.*, **B283**, 624.
- Silk, J., and Vilenkin, A. 1984, *Phys. Rev. Lett.*, **53**, 1700.
- Stebbins, A., Brandenberger, R., Veeraraghavan, S., Silk, J., and Turok, N. 1987, *Ap. J.*, in press.
- Szalay, A.S., and Schramm, D.N. 1985, *Nature*, **314**, 718.
- Tully, R.B. 1982, *Ap. J.*, **257**, 389.

- Turok. N. 1984, *Nucl. Phys.*, **B242**, 520.
- Turok. N. 1985, *Phys. Rev. Lett.*, **55**, 1801.
- Turok. N. 1987, private communication.
- Turok. N., and Bhattacharjee, P. 1984, *Phys. Rev. D*, **29**, 1557.
- Vachaspati. T. 1986, *Phys. Rev. Lett.*, **57**, 1655.
- Vachaspati. T., and Vilenkin, A. 1984, *Phys. Rev. D*, **30**, 2036.
- Vilenkin, A. 1985, *Phys. Rep.*, **121**, 263.
- Weinberg, D., Gott, J.R., and Melott, A.L. 1986, *Ap. J.*, in press.

## Figure Captions

Figure 1: An illustration of the tetrakaidekahedral lattice. Four segments pass into each vertex, and each segment is surrounded by three faces. Whether the segment is a string is determined by the phases of the Higgs field passing through the three faces. This cube is 4x4x4 in the units being used throughout.

Figure 2: A simple model to increase the density of infinite strings. The three lines represent three densities. In each step the density is increased by approximately a factor of two. The Brownian correlations, or more generally the overall correlation properties, of the system of infinite strings remain unchanged. The cube is 4x4x4 units as in Figure 1.

Figure 3: The ribbon model for wake production, used after the desired density has been reached. This cube is not necessarily drawn to the scale of the previous two figures. It may be larger than 4x4x4, since the segments may have already been increased in length.

Figure 4: Slices through the wake system, for wake production at various densities. Each line segment is the intersection of the depicted plane with a triangular wake. The average length of a straight segment,  $\lambda = \epsilon t$ , is labeled on each diagram. Figure 4a is a cross section of the configuration of wakes produced at  $\rho_{IS} \sim 0.40 \epsilon^{-2} \mu t^{-2}$ . This density is increased by a factor of two from the initial configuration. Figures b and c correspond to densities 1.2 and  $2.5 \epsilon^{-2} \mu t^{-2}$ , the later thought to be the more realistic density.

Figure 5: The cross section in Figure 4c (produced from a string configuration with density  $2.5 \epsilon^{-2} \mu t^{-2}$ ) is drawn to the scale of the CfA slice for a)  $h=0.5$  and b)  $h=1$ . c) CfA "slice of the Universe" (deLapparent, Geller, and Huchra 1986).

Figure 6: An illustration of a small portion of the wake distribution ( $\sim 2\lambda$ ) for  $\rho_{IS} = 2.5 \epsilon^{-2} \mu t^{-2}$ .

Figure 7: The distance to the nearest neighbor in a chosen direction vs. the 360 equally spaced angles in a plane, plotted for three perpendicular planes in a), b), and c). d). The distance to the edge of a sphere from a point halfway between its center and its edge in all directions in the plane passing through the center. e). The distance to the edge of a cube, along a diagonal plane, from its center.

Figure 8: The probability that a spherical region of radius  $r$  centered around a randomly chosen point is empty, for the wake distribution and for an equal density Poisson distribution. For comparison, the probability that a circular region of radius  $r$  in a cross section is

empty is also plotted. The horizontal scale is set by equating  $\lambda$  at  $z = 2z_{eq}$  to the average segment length. Square root of  $N$  error bars are negligible on the scale of this plot.

Figure 9: The correlation function for a distribution of an average of ten randomly located points on each triangular wake section. The number of points per section is proportional to the area of the section. The horizontal scale is set as in Figure 8. The slope of three regions of the  $\log \xi$  vs.  $\log r$  curve are marked within the distance ranges. Since the computation involved more than  $2.5 \times 10^5$  points, error bars corresponding to the square root of the number of pairs in each separation bin are negligible on the scale of this plot.

## Author's Address

Jane C. Charlton  
University of Chicago  
Astronomy and Astrophysics Center  
5640 S. Ellis Ave.  
Chicago, IL 60637

Fig. 1

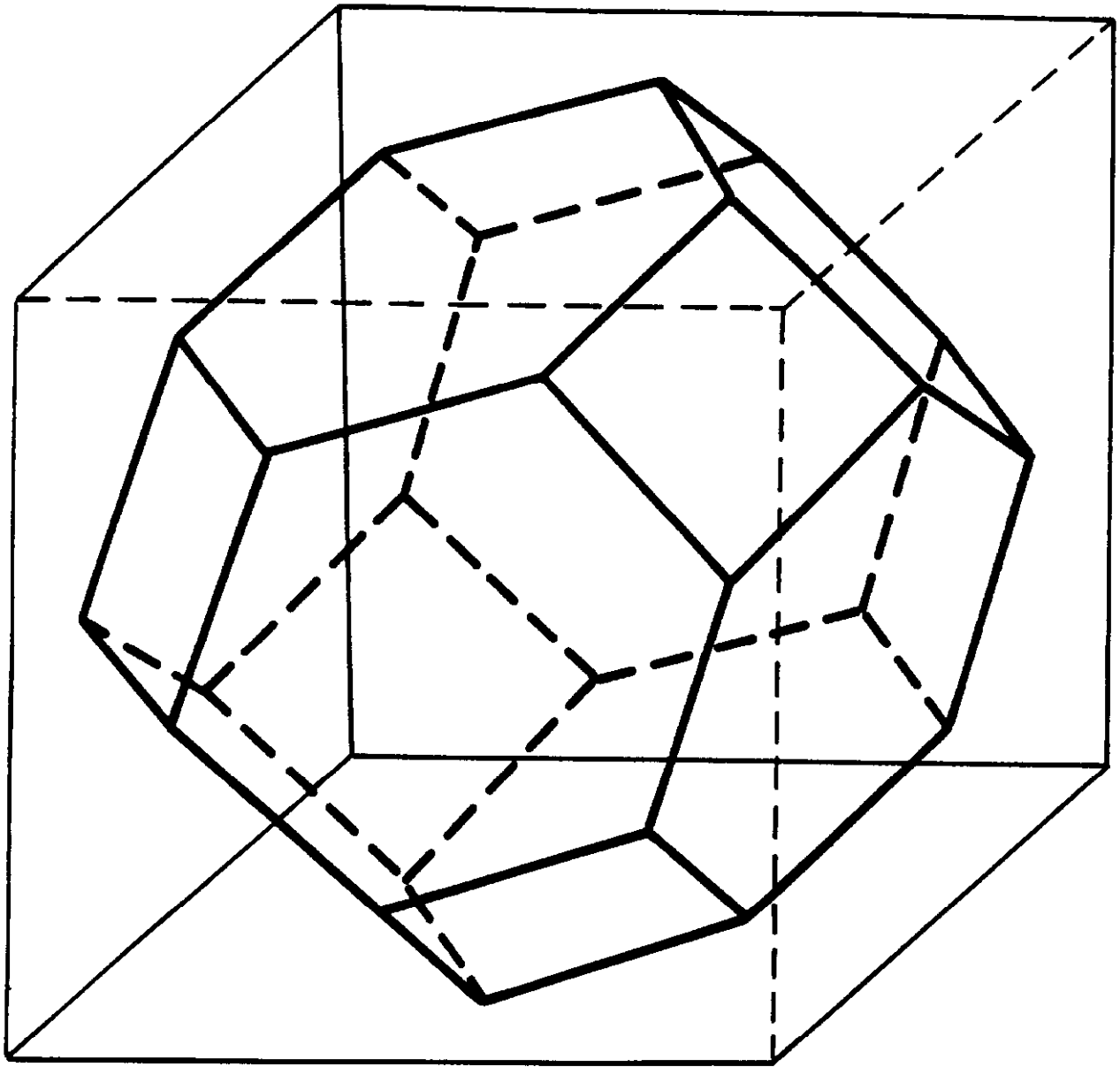
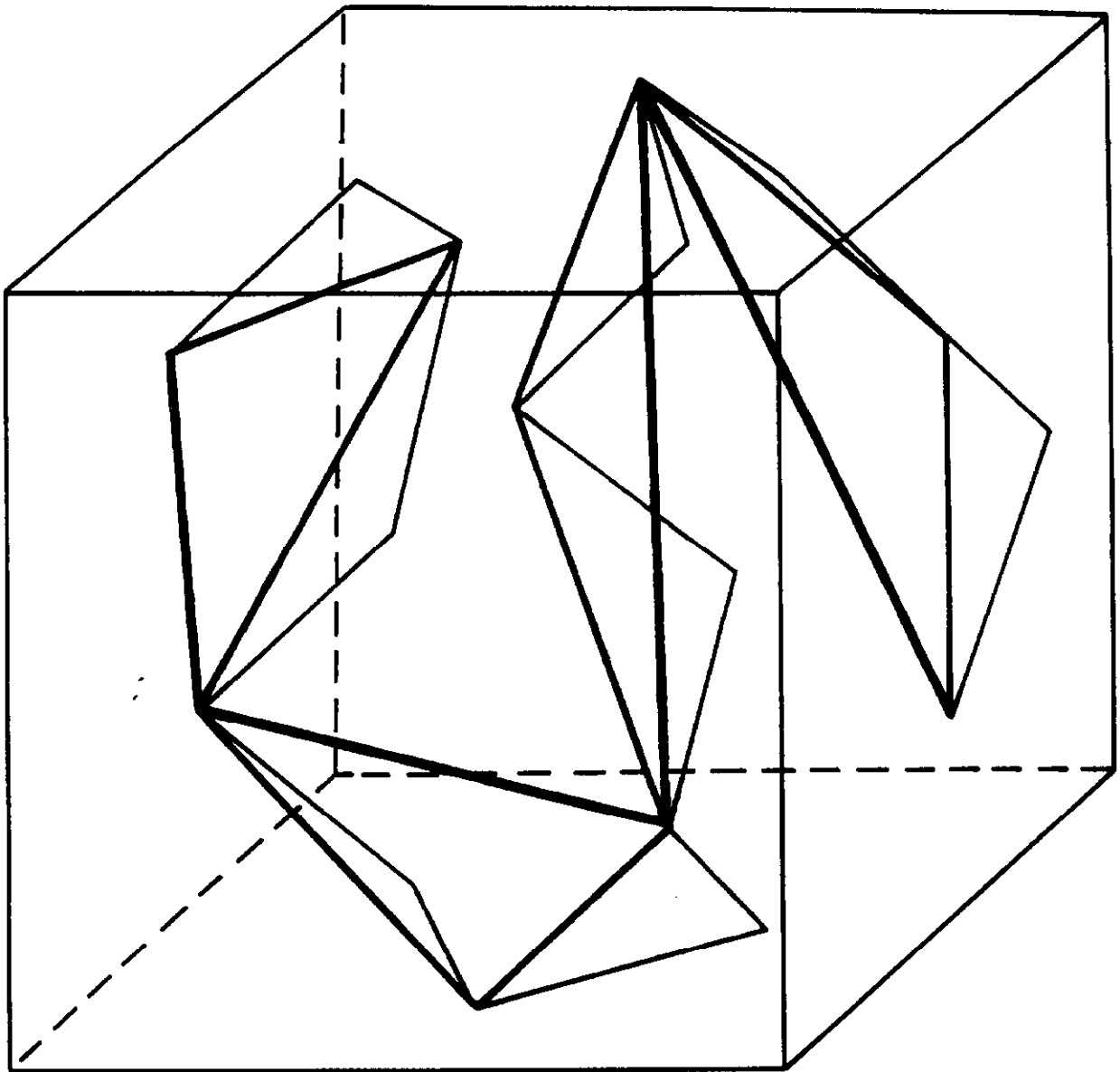
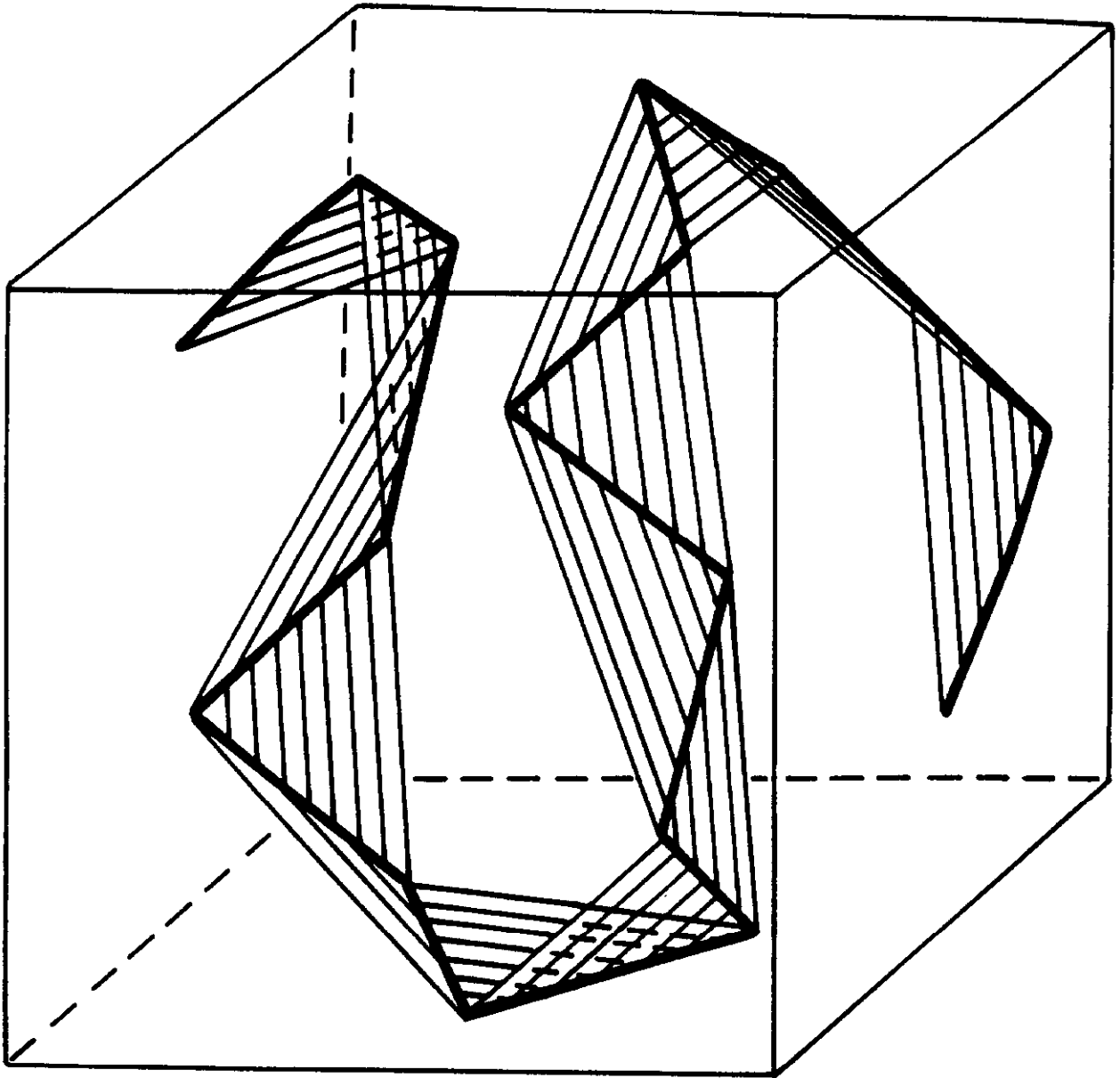


Fig. 2



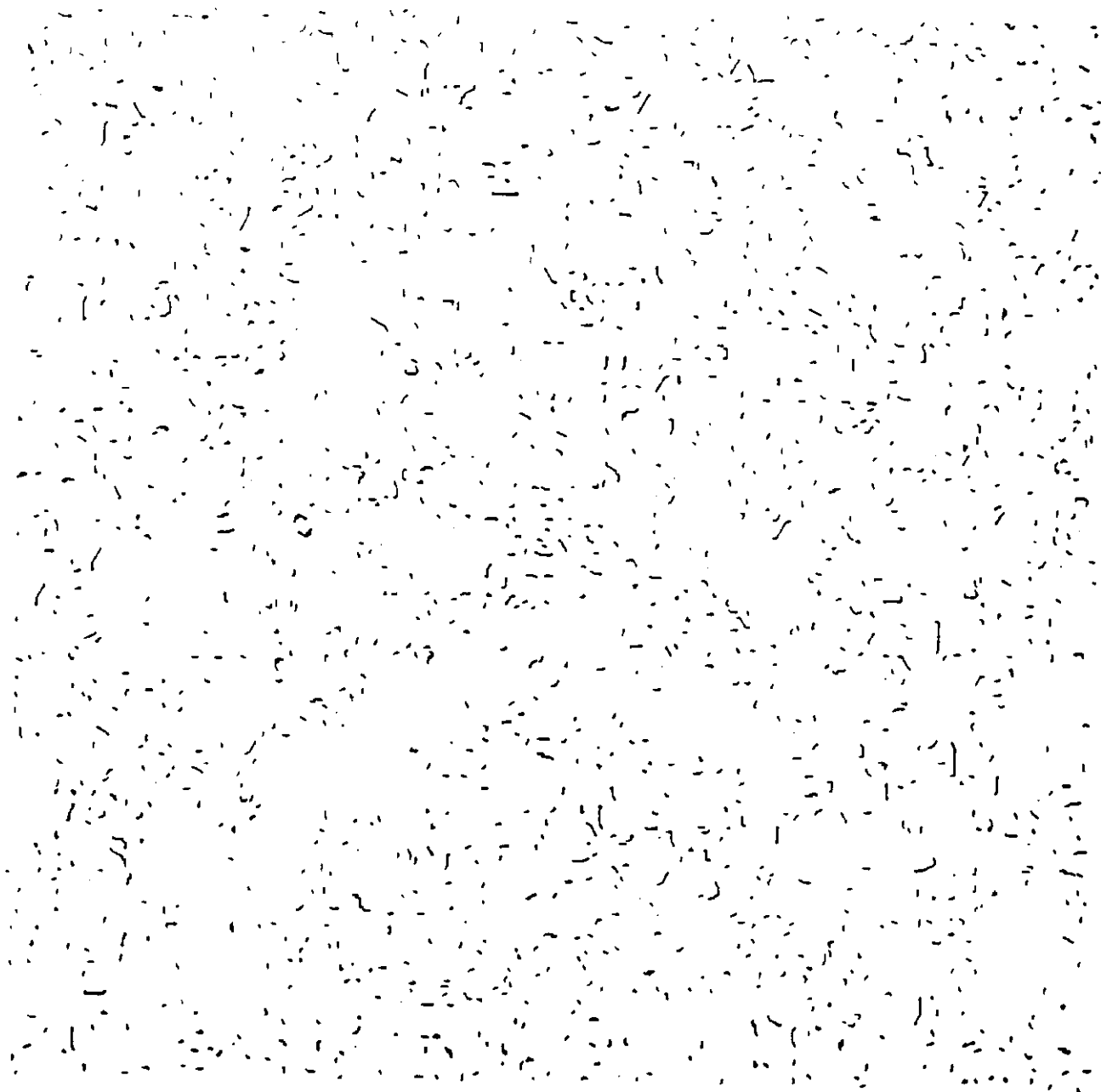
- initial configuration
- timestep one
- timestep two

Fig. 3



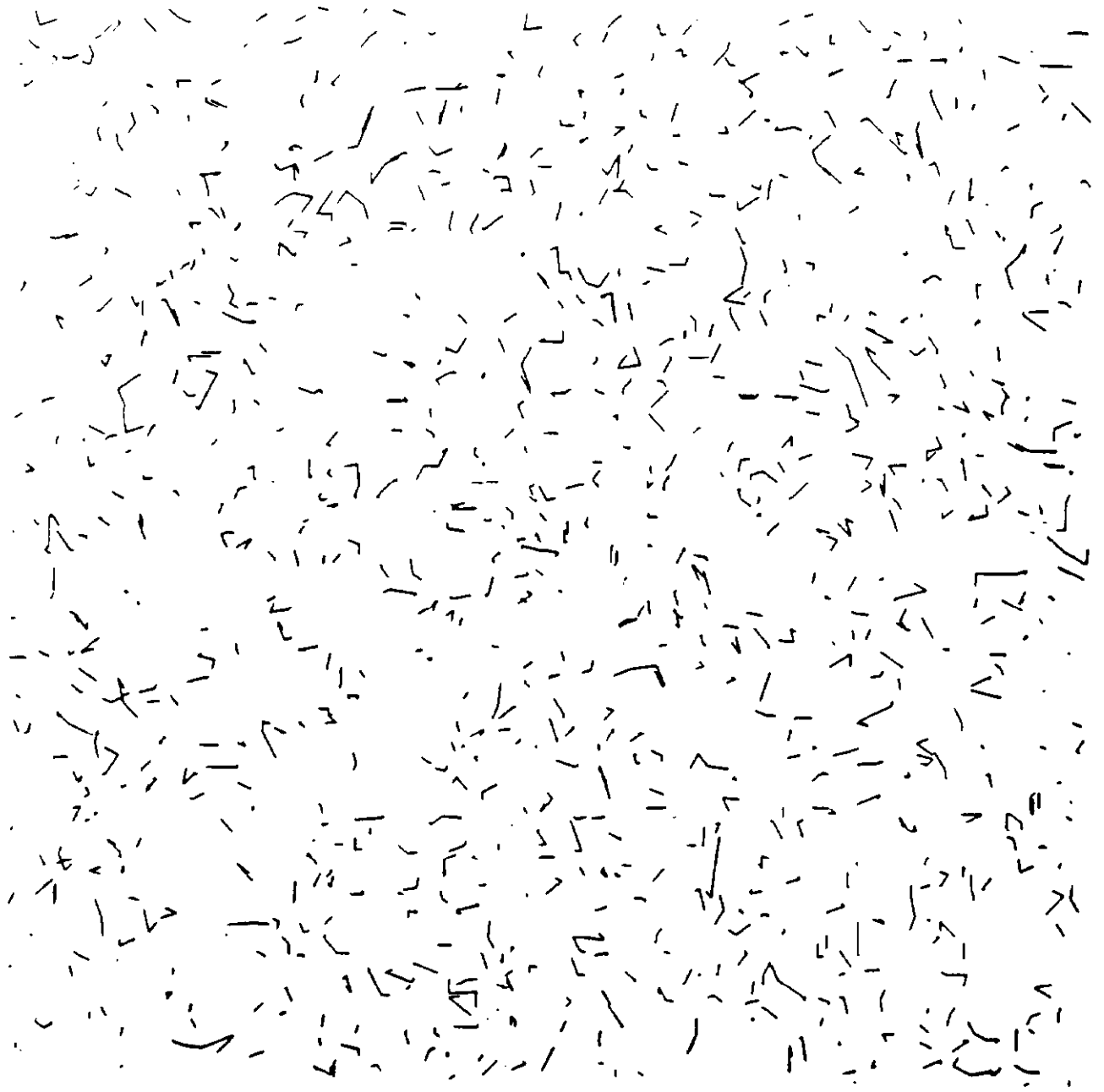
— initial string configuration

Fig. 4a



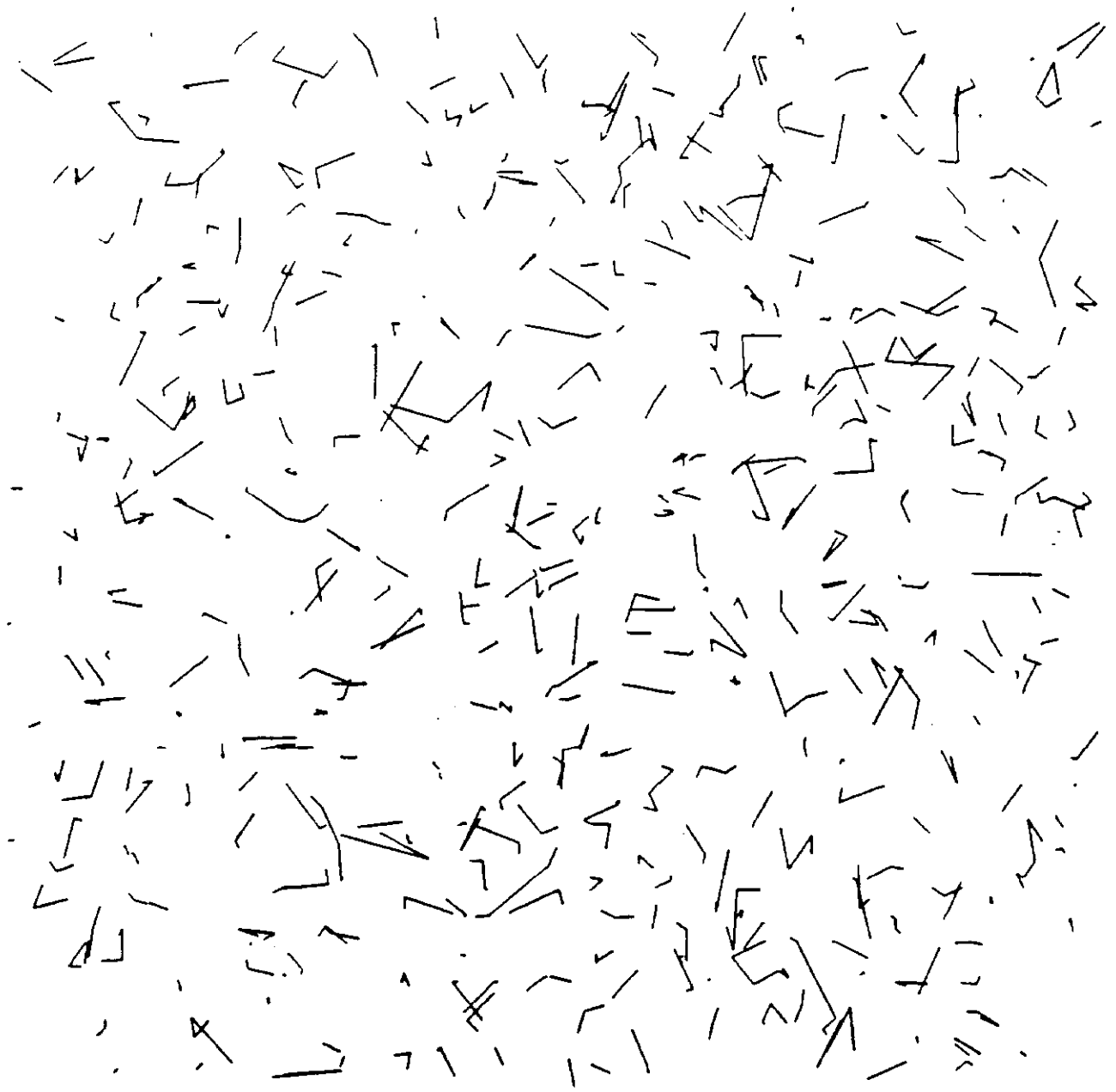
$\lambda = \epsilon t$

Fig. 4b



$$\lambda = \epsilon t$$

Fig. 4c



$\lambda = \epsilon t$  I

Fig. 5a

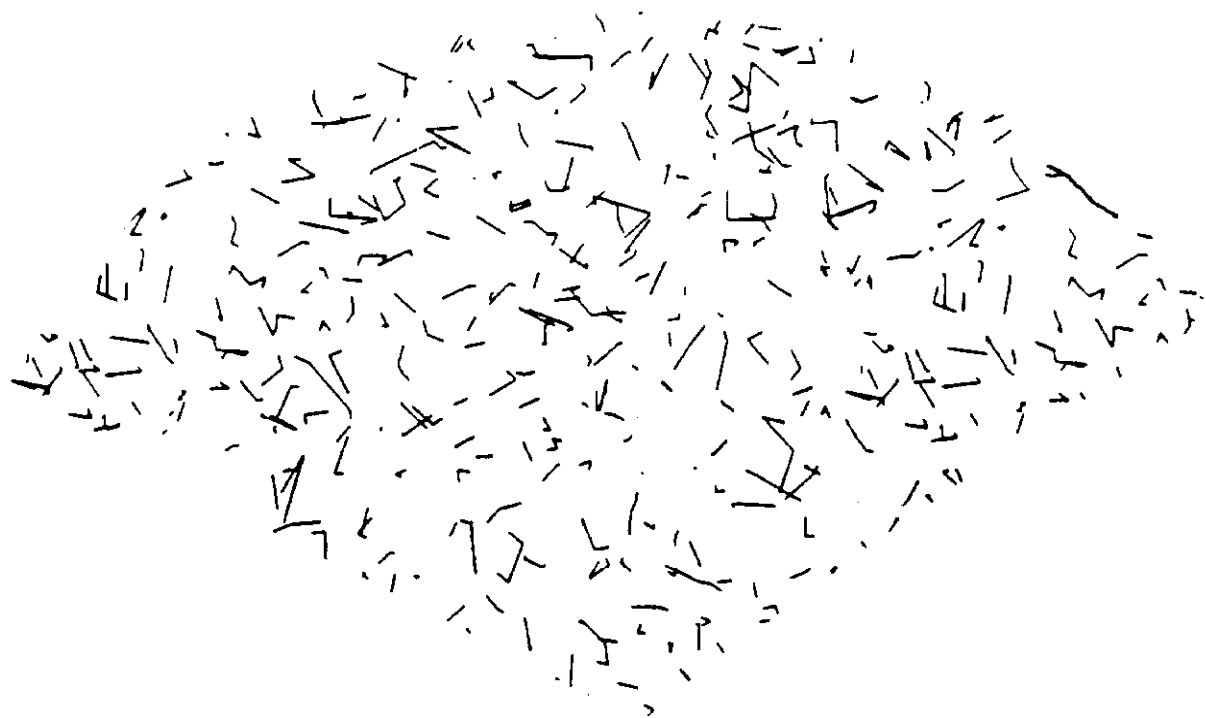


Fig. 5b

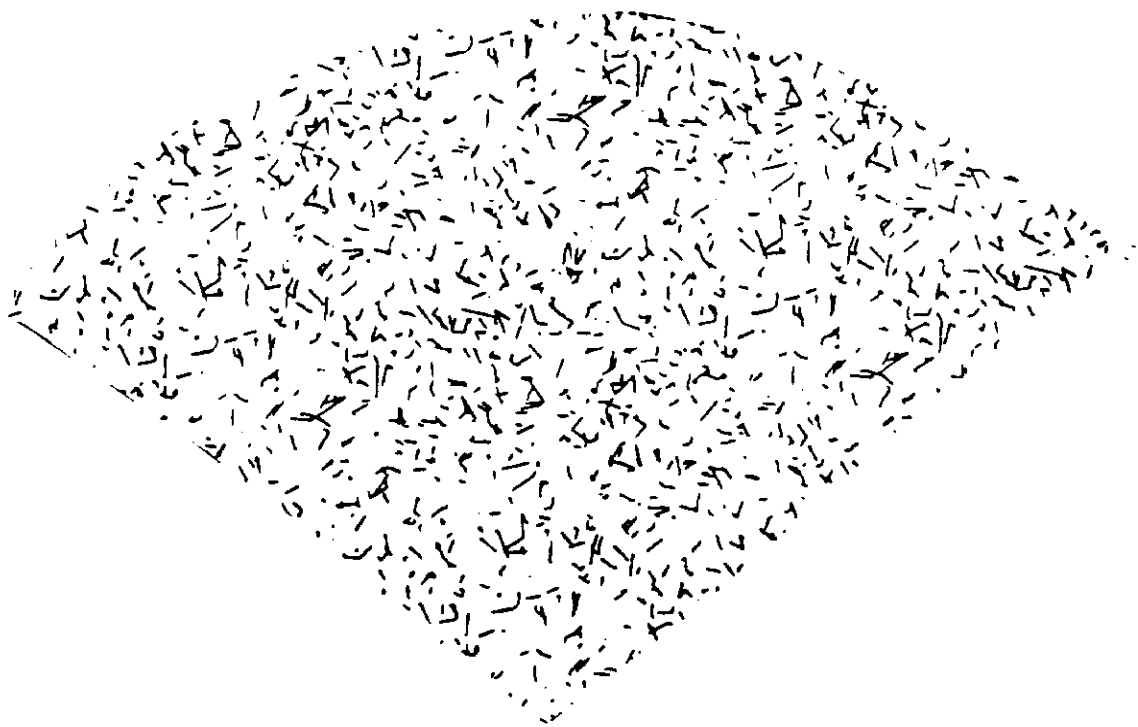


Fig. 5c

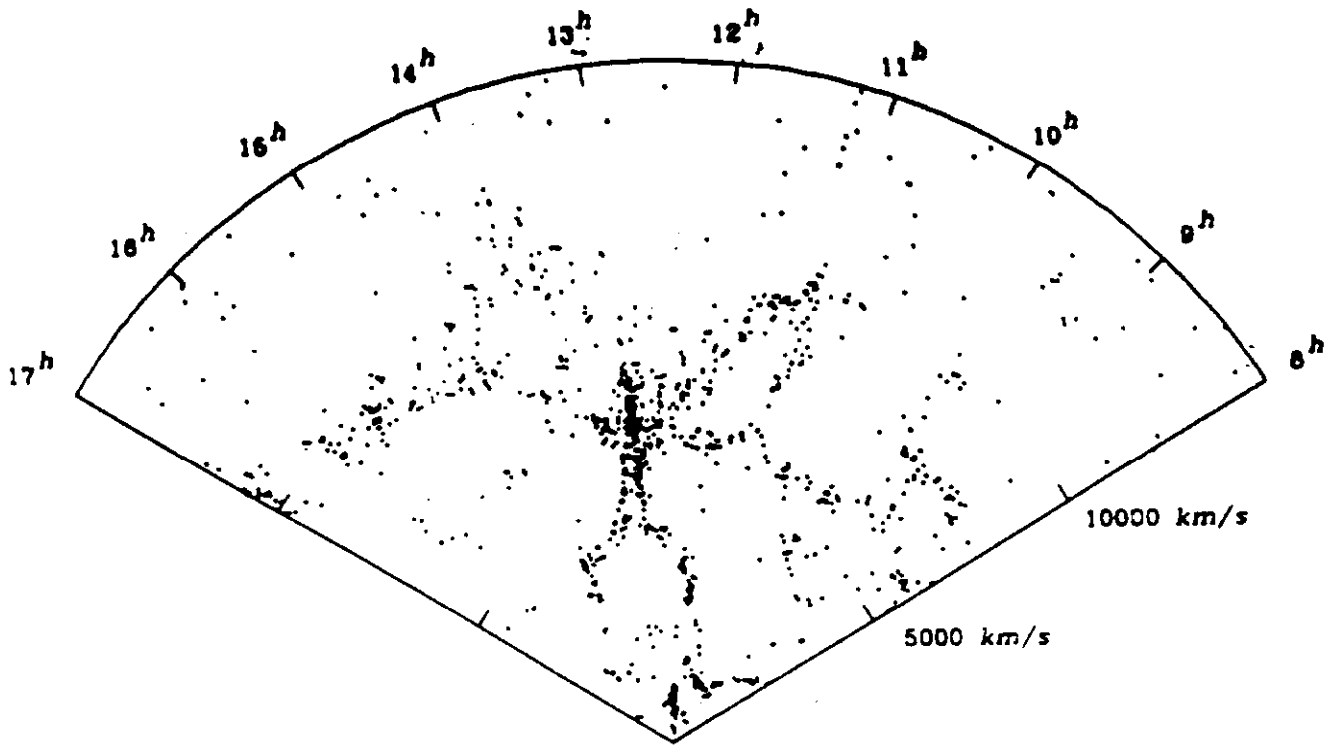
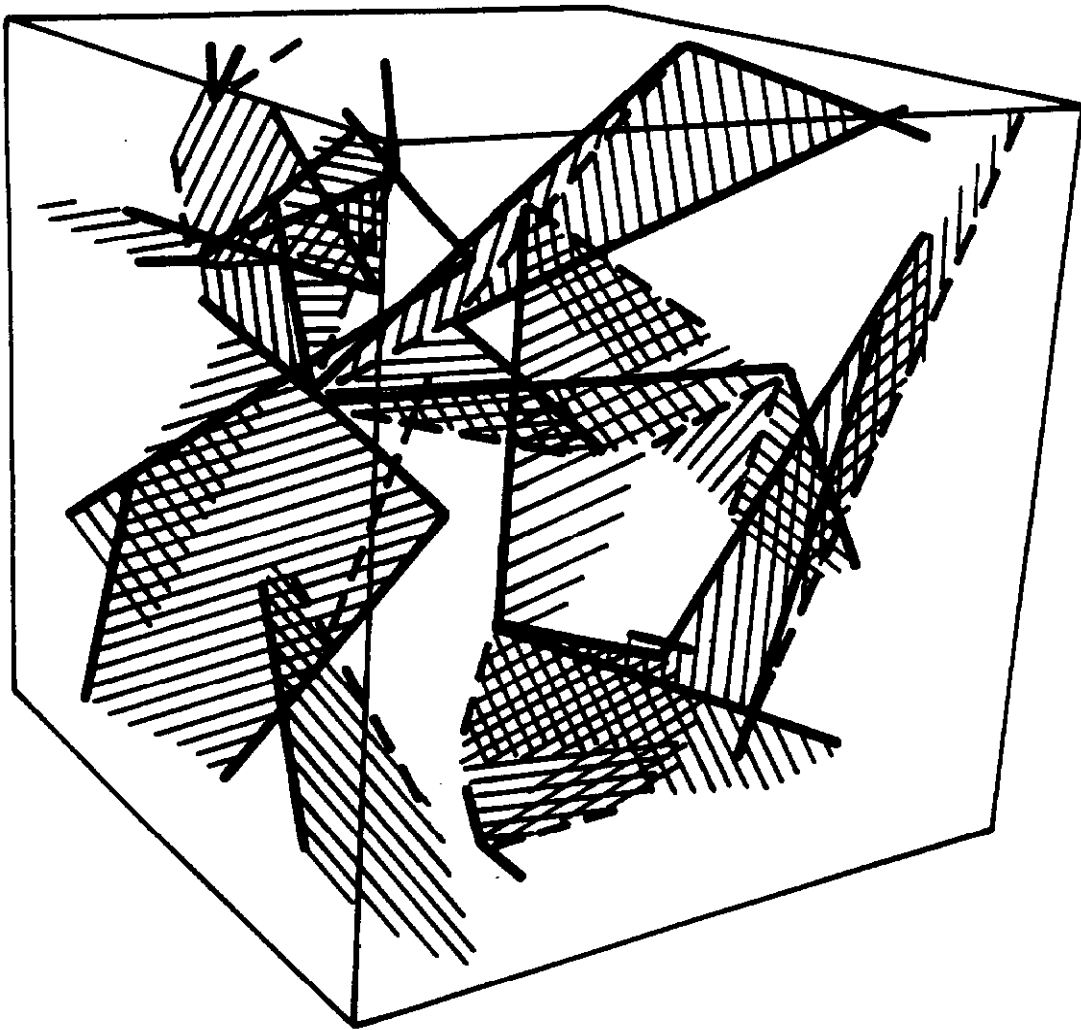


Fig. 6



Fig, 7a

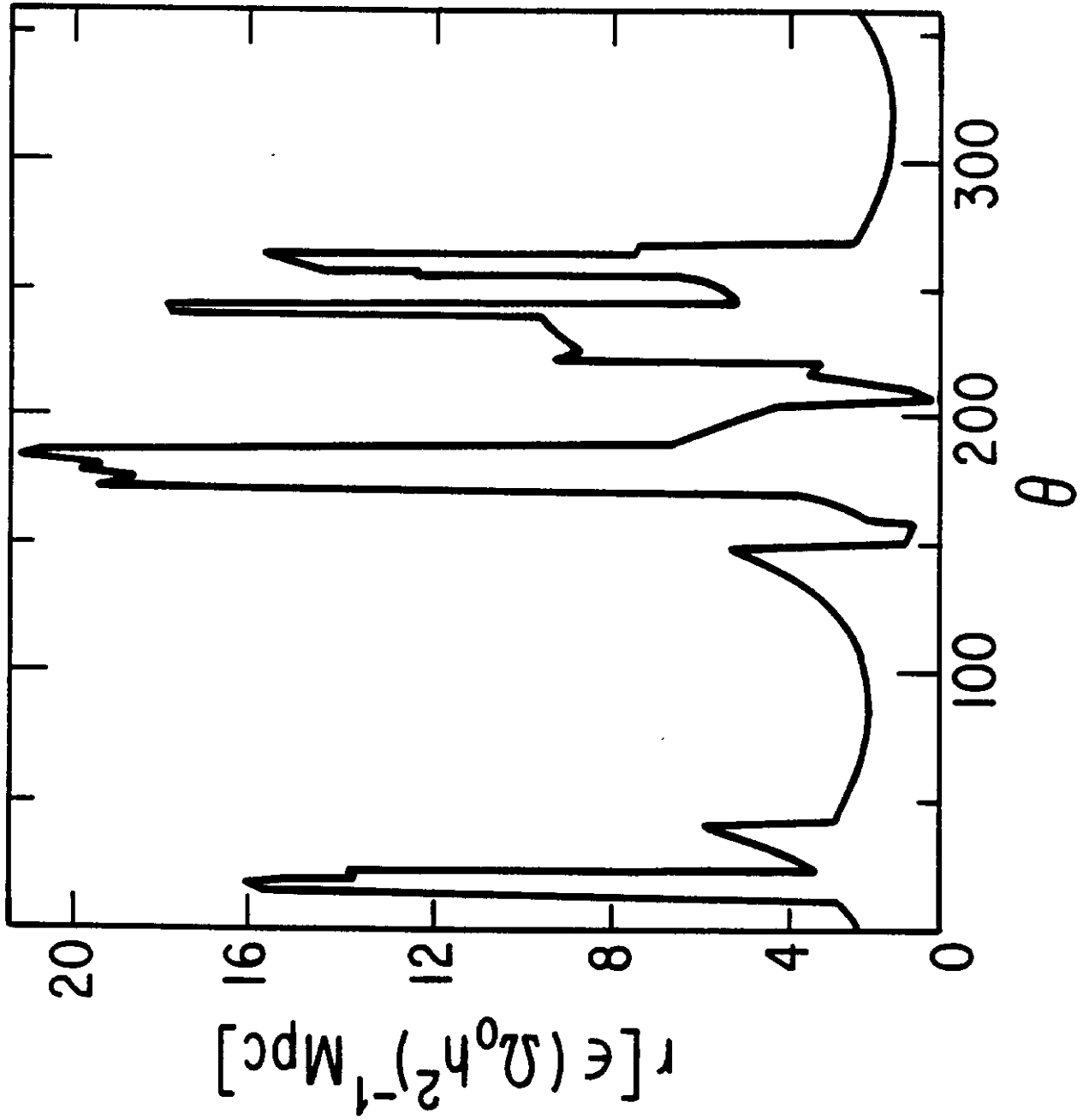


Fig. 7b

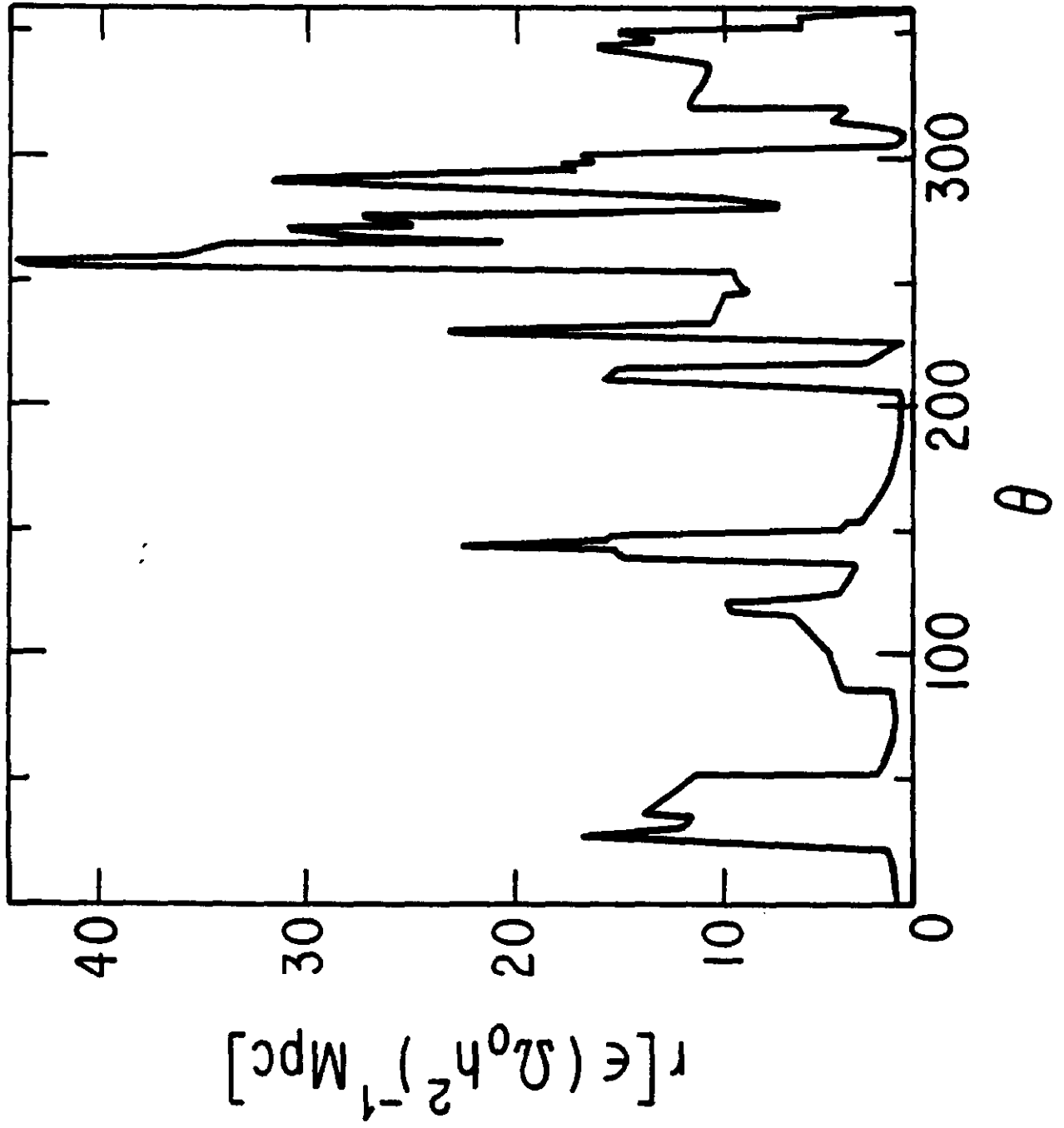


Fig. 7c

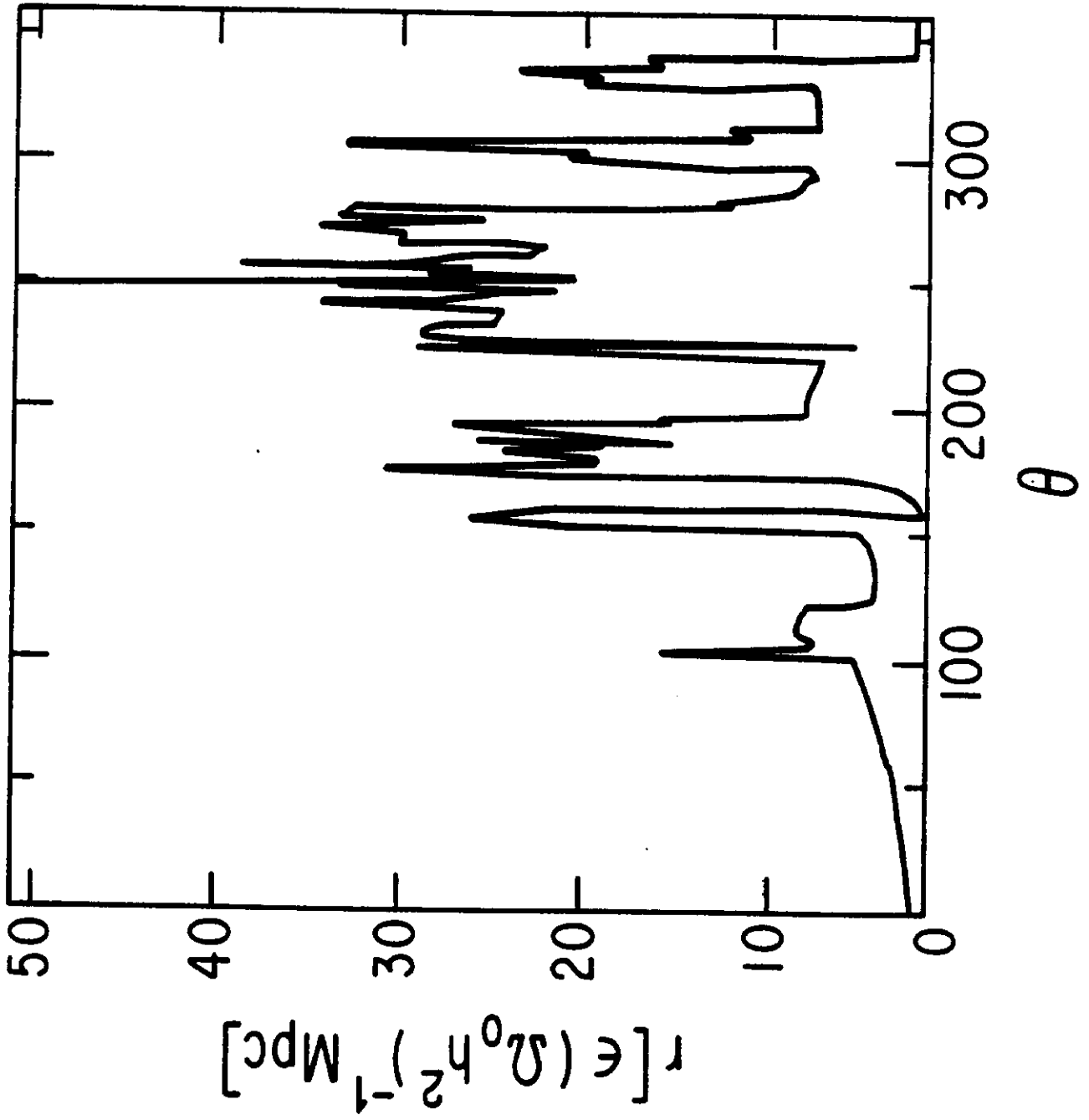


Fig. 7d

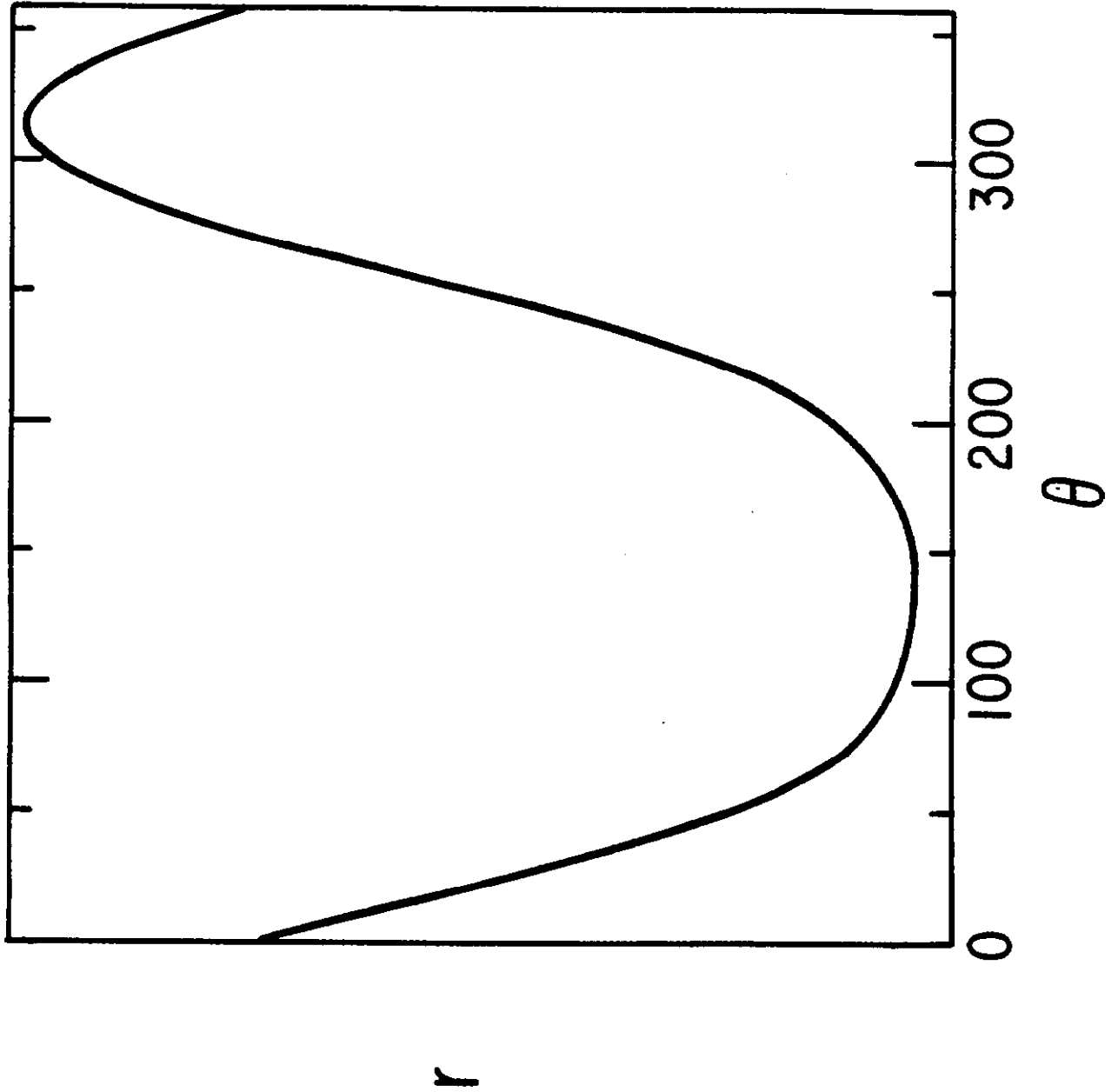
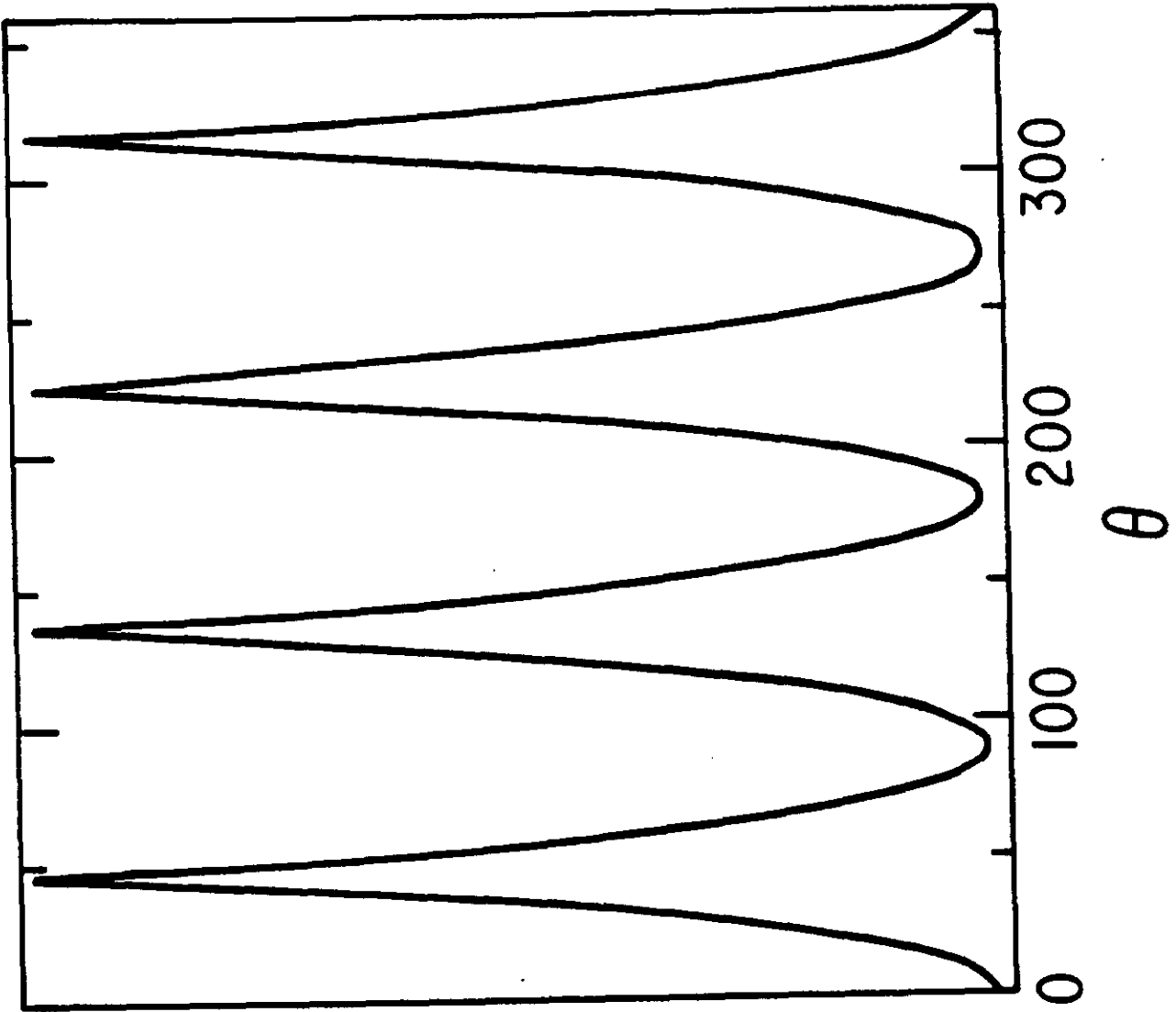


Fig. 7e



r

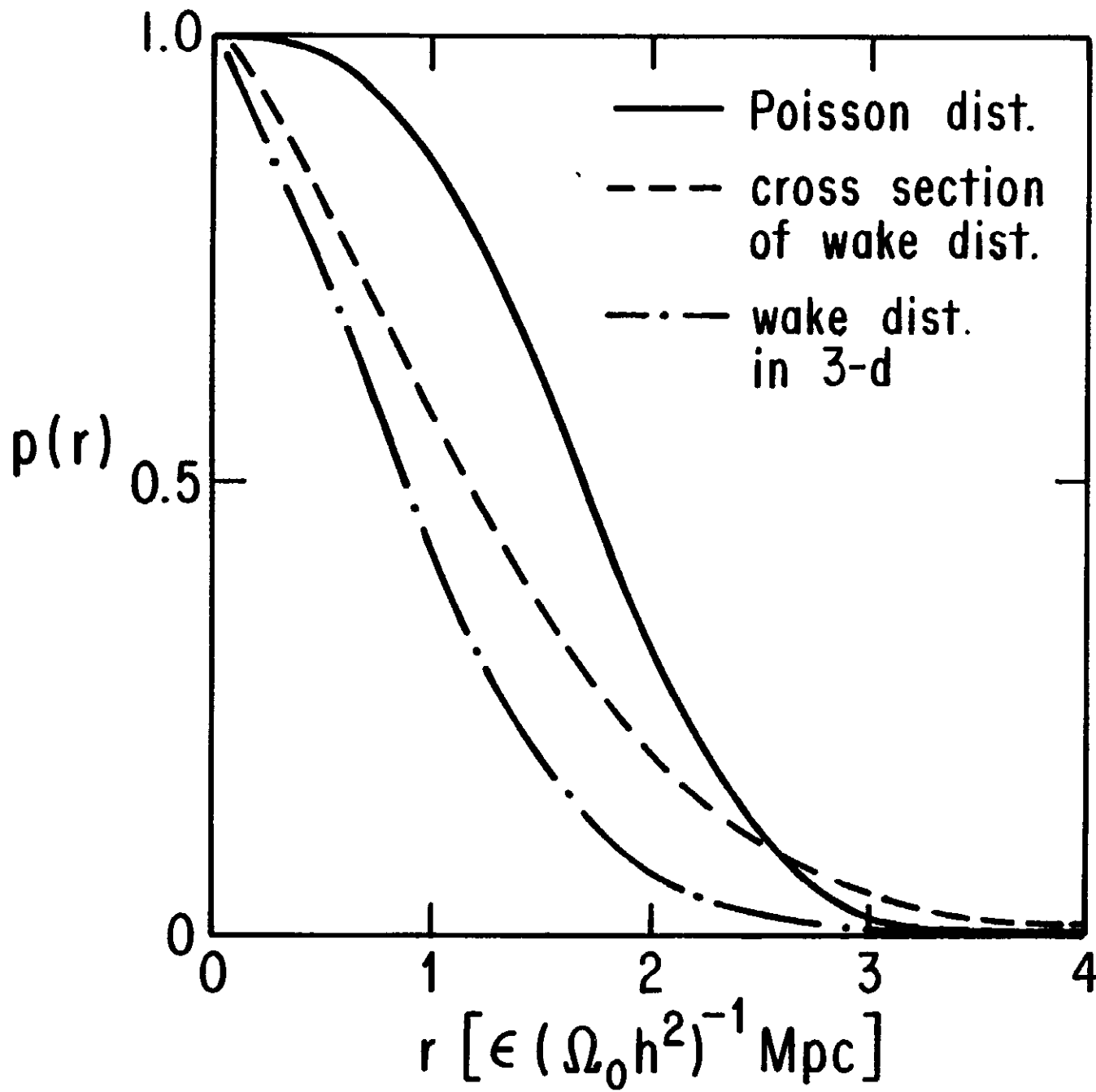


Fig. 8

Fig. 9

